

Acceleration effect of coupled oscillator systems

Toru Aonishi,¹ Koji Kurata,² and Masato Okada^{3,1}

¹*Brain Science Institute, RIKEN, 2-1 Hirosawa,
Wako-shi, Saitama, 351-0198, Japan*

²*Department of Mechanical Systems Engineering,
Faculty of Engineering, University of the Ryukyus,
Sembaru 1, Nishihara, Okinawa 903-0213, Japan*

³*ERATO Kawato Dynamic Brain Project, 2-2 Hikaridai,
Seika-cho, Soraku-gun, Kyoto 619-0288, Japan*

(Dated: November 5, 2018)

Abstract

We have developed a curved isochron clock (CIC) by modifying the radial isochron clock to provide a clean example of the acceleration (deceleration) effect. By analyzing a two-body system of coupled CICs, we determined that an unbalanced mutual interaction caused by curved isochron sets is the minimum mechanism needed for generating the acceleration (deceleration) effect in coupled oscillator systems. From this we can see that the Sakaguchi and Kuramoto (SK) model which is a class of non-frustrated mean field model has an acceleration (deceleration) effect mechanism. To study frustrated coupled oscillator systems, we extended the SK model to two oscillator associative memory models, one with symmetric and one with asymmetric dilution of coupling, which also have the minimum mechanism of the acceleration (deceleration) effect. We theoretically found that the *Onsager reaction term* (ORT), which is unique to frustrated systems, plays an important role in the acceleration (deceleration) effect. These two models are ideal for evaluating the effect of the ORT because, with the exception of the ORT, they have the same order parameter equations. We found that the two models have identical macroscopic properties, except for the acceleration effect caused by the ORT. By comparing the results of the two models, we can extract the effect of the ORT from only the rotation speeds of the oscillators.

PACS numbers: 05.45.Xt, 87.18.Sn, 75.10.Nr

I. INTRODUCTION

Coupled oscillators are of intrinsic interest in many branches of physics, chemistry, and biology. One class of coupled oscillator systems has a property that by mutual interactions, the oscillatory frequency of an individual unit is made higher (lower) than its natural frequency. This phenomenon is called the "acceleration (deceleration) effect" and is of particular interest to researchers in the biological branch of mathematics [1, 2]. However, we still do not have a clear understanding of the acceleration (deceleration) effect; we need to clarify the basic mechanism of this effect in coupled oscillator systems.

In the first part of this paper, we treat general oscillator models coupled weakly by general coupling terms according to Ermentrout [3], and we derive one-dimensional phase equations from original equations of high-dimensional dynamics. Then, we apply this general method to the radial isochron clock (RIC), which has very simple oscillator dynamics on \mathbf{R}^2 , i.e., a unit circle stable orbit. Next, we develop a curved isochron clock (CIC) by modifying the RIC, and we derive one-dimensional phase equations from coupled CICs. The CIC also has a unit circle stable orbit. We demonstrate that the CIC is a very simple model that provides a clean example of the acceleration (deceleration) effect caused by diffusion coupling. Our analysis shows that the Sakaguchi and Kuramoto (SK) model [4], which is a mean field model of coupled oscillators, has the minimum mechanism of the acceleration (deceleration) effect deeply related to coupled CICs. The SK model is not frustrated, so we need to study how frustrated interactions affect the frequency of oscillator systems.

In the next part of this paper, we propose a mean field theory that can treat a general class of frustrated coupled oscillator systems and use it to clarify the mechanism of the acceleration (deceleration) effect in frustrated coupled oscillators. We found that the *Onsager reaction term* (ORT), which describes the effective self-interaction, plays a key role in the effect. The ORT is of great importance in obtaining a physical understanding of frustrated random systems, because the presence of such an effective self-interaction is one of the characteristics that distinguish frustrated and non-frustrated systems of this types. For equilibrium systems, we can rigorously evaluate the effect of the ORT by using the Thouless-Anderson-Palmer (TAP) framework [5] and/or by using the replica method [6]. However, we cannot directly apply these systematic methods to non-equilibrium coupled-oscillator systems. While we can define a formal Hamiltonian function on such systems,

Perez and Ritort demonstrated that the ground states of such a Hamiltonian are not stationary states of the dynamics [7]. Therefore, it is impossible to construct a theory based on free energy for such systems. Consequently, to evaluate the macroscopic quantities in such systems that include an ORT, *self-consistent signal-to-noise analysis* (SCSNA), which can be applied to systems without a Hamiltonian function, has been used [8]. The mathematical treatment of this method is similar to that of the cavity method [5]. Results obtained using SCSNA have been consistent with those using the replica method, but this method includes a few heuristic steps. While SCSNA has produced some interesting results, they have not been sufficient to give a complete understanding of frustrated systems. Consequently, many fundamental theoretical questions remain in the study of such systems. In fact, even the existence of the type of self-interaction that can be described by the ORT is the subject of some debate [9, 10].

Here, we consider two oscillator associative memory models, one with symmetric and one with asymmetric dilution of coupling. These two models use are ideal for evaluating the effect of the ORT because, with the exception of the ORT, they have the same order parameter equations. The theory we present reveals a non-trivial phenomenon: oscillator rotation in a symmetric diluted model is faster (slower) than that in an asymmetric diluted model, even if the two models have identical macroscopic properties. Therefore, by comparing the results of the two models, we can extract the effect of the ORT from only the rotation speed of the oscillators.

As the random dilution of coupling in associative memory models is equivalent to the random coupling noise in the thermodynamic limit, as revealed by previously described theories of equilibrium systems [11, 12, 13], the present model is reduced to one for glass oscillators [14] in the limit of strong dilution. Therefore, the theory we propose covers two types of frustrated systems, the oscillator associative memory model and the glass oscillator model. Such models are typical frustrated non-equilibrium systems with large degrees of freedom.

In uniformly coupled oscillators, there is a unique stable state, i.e., the ferromagnetic state in the phase space. In random systems, there are many stable states in the phase space (ferromagnetic phases and glass phases). Our theory describes the mutual entrainment in the ferromagnetic phases (memory retrieval), in which most of the oscillators are synchronized by the strong mutual interaction. If the memory retrieval process is unsuccessful, the system

is in the glass phase (spurious memory retrieval), and in this phase, the system causes quasi-entrainment [14], which is regarded as weak entrainment compared to that in the ferromagnetic phase. Unfortunately, it is difficult to theoretically analyze the glass states of non-equilibrium systems because we have not yet developed sufficient theoretical tools to capture the complicated structures of the glass state in non-equilibrium systems. Therefore, instead of using theoretical analyses, we have numerically studied quasi-entrainment in the glass phase [14]. We found that the distribution of local fields takes a "volcanic" form in the glass phase [14], which implies an outbreak of the ergodicity breaking with the ultrametric structure of the glass state related to the replica-symmetry breaking.

A serious problem with using attractor-type networks for solving optimization problems is detecting being trapped in a meta-stable state during the relaxation process. Results obtained from analyzing memory retrieval and spurious memory retrieval have shown that it is possible to determine whether the retrieval process is successful or not by using information about the synchrony/asynchrony. This means that we can apply non-equilibrium systems to optimization problems in order to detect meta-stable states.

II. PHASE EQUATION

In this section, we use the method of Ermentrout [3] to derive a phase equation for coupled oscillators. First, let us consider the following isolated limit cycle oscillator:

$$\frac{d\mathbf{x}}{dt} = \mathbf{F}(\mathbf{x}), \quad \mathbf{x} \in \mathbf{R}^n, \quad \mathbf{F} : \mathbf{R}^n \rightarrow \mathbf{R}^n. \quad (1)$$

We assume this system has a stable periodic solution $\Phi(t)$ with period 2π that satisfies

$$\Phi'(t) = \mathbf{F}(\Phi(t)), \quad \Phi(t) = \Phi(t + 2\pi). \quad (2)$$

This equation is autonomous or invariant to shifts in the time domain, so $\Phi(t + \phi)$ is also a solution for any $\phi \in \mathbf{R}/2\pi$. In other words, the periodic solution is irresistant to a temporal shift while it conserves a fixed orbit (neutral stability). This is referred to as "orbit stability". Here, ϕ stands for the "phase" of the periodic solution.

If we modulate the time constant,

$$(1 - \varepsilon\omega) \frac{d\mathbf{x}}{dt} = \mathbf{F}(\mathbf{x}), \quad (3)$$

this system has a periodic solution with period $2\pi(1 - \varepsilon\omega)$, which can be expressed as

$$\mathbf{x}(t) = \Phi\left(\frac{t}{1 - \varepsilon\omega}\right), \quad (4)$$

where $1 \gg \varepsilon > 0$. When $\omega > 0$, the period of this system is slightly shorter than 2π .

Next, we consider the high-dimensional dynamics of coupled oscillator systems:

$$(1 - \varepsilon\omega_i) \frac{d\mathbf{x}_i}{dt} = \mathbf{F}(\mathbf{x}_i) + \varepsilon\mathbf{p}_i, \quad i = 1, \dots, N, \quad (5)$$

$$\mathbf{p}_i = \sum_{j(\neq i)}^N \mathbf{V}_{ij}(\mathbf{x}_i, \mathbf{x}_j), \quad (6)$$

$$\mathbf{x}_i \in \mathbf{R}^n, \quad \mathbf{V}_{ij} : \mathbf{R}^n \times \mathbf{R}^n \rightarrow \mathbf{R}^n, \quad (7)$$

where \mathbf{x}_i is a configuration variable of the i -th oscillator (with a total of N oscillators). The $\varepsilon\mathbf{p}_i$ is the perturbation, i.e., the coupling term, which is the sum of \mathbf{V}_{ij} ($i, j = 1, \dots, N$) representing the interaction from unit j to unit i . If $\varepsilon\mathbf{p}_i = 0$, each oscillator continues rotating on a limit-cycle orbit individually. The $\varepsilon\omega_i$ denotes the fluctuation in the individual natural frequency.

If ε is sufficiently small, the components of the perturbation that breaks the shape of the orbit are suppressed by the stability of the solution. However, the component of the perturbation that shifts the phase cannot be suppressed, causing the phase to move to the most "comfortable" position.

The solution of a perturbed system (5) can be represented as

$$\mathbf{u}_i(t) = \Phi(t + \phi_i(\tau)) + \varepsilon\tilde{\mathbf{u}}_i(t), \quad \tau = \varepsilon t, \quad (8)$$

where ϕ_i is the phase of the i -th oscillator (with a total of N oscillators), τ denotes a slowly varying time, and $\varepsilon\tilde{\mathbf{u}}_i$ is a fluctuation caused by the perturbation. In the following derivation, τ and ϕ_i are considered to be approximately constant within a period.

By substituting Eq. (8) into Eq. (5), expanding a polynomial around $\varepsilon = 0$, and neglecting the higher order terms, we obtain

$$\Phi'(t + \phi_i(\tau)) \left(\omega_i - \frac{d\phi_i}{d\tau} \right) + \sum_{j(\neq i)}^N \mathbf{V}_{ij}(\Phi(t + \phi_i(\tau)), \Phi(t + \phi_j(\tau))) = L_{\phi_i} \tilde{\mathbf{u}}_i, \quad (9)$$

$$L_{\phi_i} = \frac{d}{dt} - D\mathbf{F}(\Phi(t + \phi_i)), \quad (10)$$

Thus, we derive the following phase equation describing the slow dynamics of the phase-locking.

$$\frac{d\phi_i}{d\tau} = \omega_i + \sum_{j(\neq i)}^N \Gamma_{ij}(\phi_j - \phi_i), \quad (17)$$

where $\Gamma_{ij}(\phi) = \langle \Phi^*(t), \mathbf{V}_{ij}(\Phi(t), \Phi(t + \phi)) \rangle / \langle \Phi^*(t), \Phi'(t) \rangle$. $\Gamma_{ij}(\phi)$ is referred to as "coupling function", and ω_i represents the natural frequency of unit i . By using the formal multiple-scale perturbation method, we reduce the high-dimensional dynamics of oscillators to a low-dimensional representation.

III. ACCELERATION EFFECT IN DIFFUSIONALLY COUPLED OSCILLATORS (TWO-BODY SYSTEM)

In this section, we treat general oscillator models coupled weakly by diffusional coupling terms. The general theory is applied to the radial isochron clock (RIC) and curved isochron clock (CIC). Note that RIC and CIC belong to a class of the Stuart-Landau oscillator [15]. By analyzing two-body systems of coupled RICs and coupled CICs, we clarify the general mechanism of the acceleration (deceleration) effect in coupled oscillator systems.

We consider a system of two oscillators coupled by weak diffusion:

$$\begin{cases} (1 - \varepsilon\omega_1) \frac{d\mathbf{x}_1}{dt} = \mathbf{F}(\mathbf{x}_1) + \varepsilon\sigma(\mathbf{x}_2 - \mathbf{x}_1), \\ (1 - \varepsilon\omega_2) \frac{d\mathbf{x}_2}{dt} = \mathbf{F}(\mathbf{x}_2) + \varepsilon\sigma(\mathbf{x}_1 - \mathbf{x}_2), \end{cases} \quad (18)$$

where σ is the diffusion coefficient representing the coupling strength.

Based on the analysis in Section II, we can derive the following phase equation describing the slow dynamics of phase-locking.

$$\begin{cases} \frac{d\phi_1}{d\tau} = \omega_1 + \sigma\Gamma(\phi_2 - \phi_1), \\ \frac{d\phi_2}{d\tau} = \omega_2 + \sigma\Gamma(\phi_1 - \phi_2), \end{cases} \quad (19)$$

where $\Gamma(\phi) = \langle \Phi^*(t), \Phi(t + \phi) - \Phi(t) \rangle / \langle \Phi^*(t), \Phi'(t) \rangle$.

In the special case, these two oscillators are mutually locked and are accelerated (decelerated) by the effect of diffusional coupling. We term this phenomenon "the acceleration (deceleration) effect". We next derive the conditions for it.

We can express phase-locking solution of Eq. (19) as

$$\phi_1(\tau) = \omega\tau + \eta_1, \quad \phi_2(\tau) = \omega\tau + \eta_2, \quad \eta = \eta_2 - \eta_1, \quad (20)$$

where ω , η_1 , and η_2 are constant. When $\sigma = 0$, the natural periods of the two oscillators are $\frac{2\pi}{1+\varepsilon\omega_1}$ and $\frac{2\pi}{1+\varepsilon\omega_2}$, respectively. On the other hand, when the two oscillators are mutually locked ($\sigma \neq 0$), their periods are equal to $\frac{2\pi}{1+\varepsilon\omega}$. Here, we assume

$$\omega_1 > \omega_2. \quad (21)$$

This assumption does not lose the generality of our theory.

To obtain the parameter regions of the acceleration (deceleration) effect, we need to define the effect. One definition for the effect is the following. If $\omega > (\omega_1 + \omega_2)/2$, the two oscillators are locked at a speed faster than their mean natural rotation speed. This condition is defined as "acceleration". If $\omega < (\omega_1 + \omega_2)/2$, the two oscillators are locked at a speed slower than their mean natural rotation speed. This is defined as "deceleration". However, in this section, we focus on more a radical situation.

If $\omega > \omega_1$, the two oscillators are locked at a speed faster than either of their natural rotation speeds. This condition is defined as "acceleration". If $\omega < \omega_2$, the two oscillators are locked at a speed slower than either of their natural rotation speeds. This is defined as "deceleration". If $\omega_2 \leq \omega \leq \omega_1$, the two oscillators are locked at a speed midway between their natural rotation speeds. This condition is called the "medium state", and it does not belong to the acceleration (deceleration) effect. In the following analyses of two-body systems, we use these more radical definitions.

By substituting Eq. (20) into Eq. (19), we obtain

$$\omega = \omega_1 + \sigma\Gamma(\eta) = \omega_2 + \sigma\Gamma(-\eta). \quad (22)$$

We can rewrite Eq. (22) as

$$\Gamma(\eta) - \Gamma(-\eta) = -\frac{\omega_1 - \omega_2}{\sigma}. \quad (23)$$

Consequently, we can graphically obtain η from Eq. (23) and then obtain ω from Eq. (22). Since, in general, Eq. (23) possesses two or more solutions consisting of stable and unstable fixed points, the following stability condition must be satisfied:

$$\sigma(\Gamma'(\eta) + \Gamma'(-\eta)) > 0. \quad (24)$$

Given Eq. (21), we obtain the following conditions for the acceleration (deceleration) effect

from Eq. (22).

$$\begin{aligned}\sigma\Gamma(\eta) > 0 : & \text{ (acceleration),} \\ \sigma\Gamma(-\eta) < 0 : & \text{ (deceleration),}\end{aligned}\tag{25}$$

These conditions imply that mutual couplings between two oscillators are asymmetric; that is, $\Gamma(\eta) \neq \Gamma(-\eta)$. Consequently, asymmetric mutual interaction is the essence of the acceleration (deceleration) effect.

Next, we apply this general theory to two special models: the radial isochron clock (RIC) and the curved isochron clock (CIC). In general, limit cycle oscillators have the so-called "isochron", which is defined as a set of initial states converging to a oscillatory solution with a common phase.

The RIC is one of the simplest oscillators on \mathbf{R}^2 , which has a unit circle orbit with period 2π and isochron sets that are half-lines radiating from the origin (see Figure 1(a)). RIC is expressed in the polar coordinate system as

$$\begin{cases} \dot{r} = r(1 - r^2) \\ \dot{\theta} = 1 \end{cases}.\tag{26}$$

We schematically study two-body systems with diffusional coupling; these systems consist of a faster and a slower RIC. As shown in Figure 1(a), the two oscillators pull each other due to the effect of their diffusional coupling. One is pulled backward from the isochron, while the other is pulled forward. As a result, one is decelerated and the other is accelerated throughout a period. Thus, the two oscillators are locked at a speed midway between their natural rotation speeds.

Next, we describe our proposed curved isochron clock (CIC), which is defined as

$$\begin{cases} \dot{r} = r(1 - r^2) \\ \dot{\theta} = 1 + \omega(r) \end{cases},\tag{27}$$

where $\omega(1) = 0$. The CIC has a unit circle orbit with period 2π and curved isochron sets (see Figure 1(b)). Figure 1(b) shows that if there is a phase difference, the oscillators are pulled forward from the isochron. This happens because the isochrons of the CIC intersect non-orthogonally with a limit cycle. Accordingly, the two oscillators can be accelerated throughout a period by locking them with a phase difference. Thus, we should be able to lock two oscillators at a faster speed than either of their natural rotation speeds.

This consideration can be applied to the general case of weakly diffusively coupled oscillators. However, in general, the limit cycle and isochron sets are not rotation symmetric, so the acceleration (deceleration) effect must be averaged through a period.

We next derive the coupling function of diffusively coupled CICs. A solution on the unit circle orbit is expressed in the orthogonal coordinate system as follows:

$$\Phi(t) = \begin{pmatrix} \cos t \\ \sin t \end{pmatrix}. \quad (28)$$

In this case, we can explicitly derive $\Phi^*(t)$:

$$\Phi^*(t) = \frac{1}{2\pi} \begin{pmatrix} -\sin t \\ \cos t \end{pmatrix} + \frac{\omega'(1)}{4\pi} \begin{pmatrix} \cos t \\ \sin t \end{pmatrix}, \quad (29)$$

As a result, we obtain the coupling function:

$$\begin{aligned} \Gamma(\eta) &= \frac{1}{\cos \beta_0} (\sin(\eta + \beta_0) - \sin \beta_0), \\ \beta_0 &= \tan^{-1} \frac{\omega'(1)}{2}, \quad -\frac{\pi}{2} < \beta_0 < \frac{\pi}{2}. \end{aligned} \quad (30)$$

Here, β_0 is derived from the intersection angle between the isochron and the orbit. If $\beta_0 = 0$, Eq. (30) corresponds to weakly coupled RICs. Consequently, this phase reduction maintains the essence of the acceleration (deceleration) effect. We can study the acceleration (deceleration) phenomenon of diffusively coupled CICs by analyzing Eq. (30). The parameter regions of the acceleration (deceleration) effect, which are obtained from the conditions defined by Eqs. (23), (24), and (25) are as follows.

If $\sigma > 0$,

$$\begin{aligned} \sin \eta &= -\frac{\omega_1 - \omega_2}{2\sigma}, \quad -\pi/2 < \eta < 0, \\ &\begin{cases} -\frac{\pi}{2} < \beta_0 < \frac{-\pi-\eta}{2} & \text{(acceleration)} \\ \frac{\pi+\eta}{2} < \beta_0 < \frac{\pi}{2} & \text{(deceleration)} \end{cases}. \end{aligned} \quad (31)$$

If $\sigma < 0$,

$$\begin{aligned} \sin \eta &= -\frac{\omega_1 - \omega_2}{2\sigma}, \quad \pi/2 < \eta < \pi, \\ &\begin{cases} \frac{\pi-\eta}{2} < \beta_0 < \frac{\pi}{2} & \text{(acceleration)} \\ -\frac{\pi}{2} < \beta_0 < \frac{-\pi+\eta}{2} & \text{(deceleration)} \end{cases}. \end{aligned} \quad (32)$$

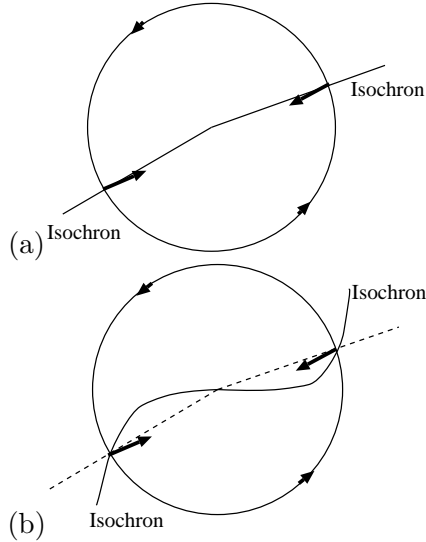


FIG. 1: (a) Schematic diagram of two diffusionally coupled RICs and (b) of two diffusionally coupled CICs.

Figure 2 shows a phase diagram of the acceleration (deceleration) effect of two diffusionally coupled CICs.

Sakaguchi and Kuramoto proposed a mean field model (the SK model) of coupled oscillators [4]. The acceleration (deceleration) effect is also observed in the SK model from the point of view of our proposed theory. The SK model is expressed by

$$\frac{d\phi_i}{d\tau} = \omega_i + \frac{J}{N} \sum_{j(\neq i)}^N \sin(\phi_j - \phi_i + \beta_0), \quad (33)$$

where ϕ_i is the phase of the i -th oscillator (with a total of N oscillators), and ω_i represents its natural frequency. The quantity J represents the strength of the mutual coupling. The quantity β_0 in Eq. (33) represents a uniform bias. Since Eq. (33) can be interpreted as a system of weakly coupled CICs, β_0 represents the intersection angle between the isochron and the orbit, as described above. Due to the effect of the bias caused by the curved isochron sets, the mutual interaction between a pair of oscillators is asymmetric. Such an unbalanced mutual interaction is the mechanism of the acceleration (deceleration) effect. Therefore, we can conclude that the SK model has the minimum mechanisms for the acceleration (deceleration) effect related to curved isochron sets. As the SK model is not frustrated, we need to study frustrated coupled oscillator systems.

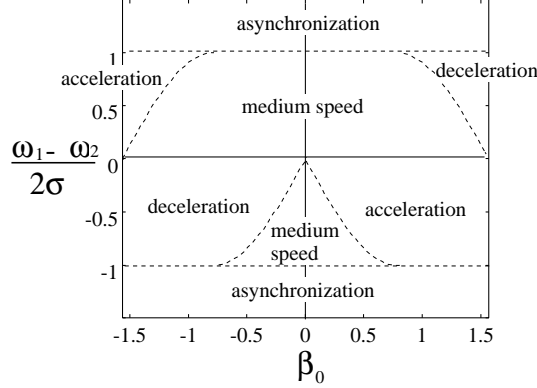


FIG. 2: Parameter region of acceleration (deceleration) effect of two diffusively coupled CICs.

IV. FRUSTRATED COUPLED OSCILLATOR SYSTEMS

In this section, we extend the SK model to frustrated coupled oscillator systems with large degrees of freedom and describe the mechanism of the acceleration (deceleration) effect unique to frustrated coupled oscillators.

In general, frustrated systems differ from ferromagnetic ones in that they have the *Onsager reaction term* (ORT). Here, we focus on the effect of the ORT on the acceleration (deceleration) that exists only in frustrated globally coupled oscillator systems, and in particular cannot be found in equilibrium systems. To make this effect clear, it would be best to compare two frustrated systems that, with the exception of a different quantity of the ORT, have the same order parameter equations. In addition, these systems should have a clear correspondence with an equilibrium system because the effects of the ORT are well understood in equilibrium systems.

We thus consider a system with the following form to be ideal.

$$\frac{d\phi_i}{d\tau} = \omega_i + \sum_{j(\neq i)}^N J_{ij} \sin(\phi_j - \phi_i + \beta_{ij} + \beta_0), \quad (34)$$

This simple phase equation was obtained by approximating $\Gamma_{ij}(\phi)$ in Eq. (17) to the lowest frequency component. In fact, such systems are commonly used as models of coupled oscillator systems [14, 15, 16, 17, 18]. Natural frequencies $\{\omega_i\}_{i=1,\dots,N}$ in Eq. (34) are randomly distributed with a density represented by $g(\omega)$. Also in Eq. (34), J_{ij} , and β_{ij} denote the amplitude of coupling from unit j to unit i and its delay, respectively. In the present study, we have selected the following two generalized Hebb learning rules with random dilutions

[12] to determine J_{ij} and β_{ij} :

$$K_{ij} = J_{ij} \exp(i\beta_{ij}) = \frac{c_{ij}}{cN} \sum_{\mu=1}^p \xi_i^\mu \bar{\xi}_j^\mu, \quad (35)$$

$$\xi_i^\mu = \exp(i\theta_i^\mu), \quad (36)$$

$$c_{ij} = \begin{cases} 1 & \text{with probability } c \\ 0 & \text{with probability } 1 - c \end{cases}, \quad (37)$$

where $\bar{\cdot}$ means the complex conjugate. The $\{\theta_i^\mu\}_{i=1, \dots, N, \mu=1, \dots, p}$ are the phase patterns to be stored in the present model and are assigned to random numbers with a uniform probability on the interval $[0, 2\pi]$. The μ is an index of the stored pattern, and p is the total number of stored patterns. We define parameter α (the loading rate) by $\alpha = p/N$. When $\alpha \sim O(1)$, the system is frustrated. When $\alpha = 0$, the system is equivalent to the SK model. The quantity c_{ij} is the dilution coefficient. Let $c_{ij} = 1$ if there is non-zero coupling from unit j to unit i and $c_{ij} = 0$ otherwise. The number of fan-ins (fan-outs) is restricted to $O(N)$, i.e., $c \sim O(1)$.

Here, we consider both symmetric dilution (i.e., $c_{ij} = c_{ji}$) and asymmetric dilution (i.e., c_{ij} and c_{ji} are independent random variables)[13]. The quantity β_0 in Eq. (34) represents a uniform bias. Since Eq. (34) can be interpreted as a system of weakly coupled CICs, β_0 represents the intersection angle between the isochron and the orbit, as discussed in Section III. Due to the effect of the bias caused by the curved isochron sets, the mutual interaction between a pair of oscillators is asymmetric, even if $J_{ij} = J_{ji}$ and $\beta_{ij} = -\beta_{ji}$. Such an unbalanced mutual interaction is the essence of the acceleration (deceleration) effect, because oscillators are pulled forward from the isochron, as discussed in Section III. If $\beta_0 = 0$, Eq. (34) is equivalent to weakly coupled RICs.

There is a close analogy between the phase description of coupled oscillators and the classical XY-spin model of magnetic material. If $\omega_i = 0$, $\beta_0 = 0$, $J_{ij} = J_{ji}$, and $\beta_{ij} = -\beta_{ji}$, we can define the following Lyapnov function on the system:

$$E = -\frac{1}{2} \sum_{i,j}^N J_{ij} \cos(\phi_j - \phi_i + \beta_{ij}). \quad (38)$$

This function enables us to use conventional statistical mechanics for XY-spin systems [19] to analyze coupled oscillators in the equilibrium state. Thus, this system can be mapped to an XY-spin system [12, 19]. In this way, we can make a bridge between the frustrated coupled oscillator system and the equilibrium system.

V. ORDER PARAMETER EQUATIONS

Let us consider steady states of the system in the limit $\tau \rightarrow \infty$. Our theory is based on the condition that there is one large cluster of oscillators synchronously locked at frequency Ω and the number of this cluster scales as $\sim O(N)$. Under this condition, Daido demonstrated, through a scaling plot obtained from numerical simulation, that variation in the parameter order scales as $O(1/\sqrt{N})$ in ferromagnetic systems with one large synchronous cluster [20]. We thus assume that the self-averaging property holds in our system and that the order parameters are constant in the limit $N \rightarrow \infty$. These assumptions were also used by Sakaguchi and Kuramoto [4].

Redefining ϕ_i according to $\phi_i \rightarrow \phi_i + \Omega\tau$ and substituting this into Eq. (34), we obtain

$$-\frac{d\phi_i}{d\tau} + \omega_i - \Omega = \sin(\phi_i)h_i^R - \cos(\phi_i)h_i^I. \quad (39)$$

where h_i represents the so-called "local field", which is described as

$$\begin{aligned} h_i &= h_i^R + ih_i^I = e^{i\beta_0} \sum_{j(\neq i)}^N K_{ij} s_j = e^{i\beta_0} \\ &\times \left(\sum_{\mu}^p \xi_i^{\mu} m^{\mu} + \frac{1}{N} \sum_{\mu}^p \sum_{j(\neq i)}^N \frac{c_{ij} - c}{c} \xi_i^{\mu} \bar{\xi}_j^{\mu} s_j - \alpha s_i \right), \end{aligned} \quad (40)$$

For convenience, we write $s_i = \exp(i\phi_i)$. The order parameter m^{μ} , which is the overlap between the system state $\{s_i\}_{i=1,\dots,N}$ and embedded pattern $\{\xi_i^{\mu}\}_{i=1,\dots,N}$, is defined as

$$m^{\mu} = \frac{1}{N} \sum_{j=1}^N \bar{\xi}_j^{\mu} s_j. \quad (41)$$

In the thermodynamic limit, the effect of the second term of Eq. (40), i.e. $\frac{1}{N} \sum_{\mu}^p \sum_{j \neq i}^N \frac{c_{ij} - c}{c} \xi_i^{\mu} \bar{\xi}_j^{\mu} s_j$, is equivalent to that of the effect of additive coupling noise [11, 12, 13]:

$$K_{ij} = J_{ij} \exp(i\beta_{ij}) = \frac{1}{N} \sum_{\mu=1}^p \xi_i^{\mu} \bar{\xi}_j^{\mu} + \delta n_{ij} \quad (42)$$

$$\text{Re}\delta n_{ij} \sim \mathcal{N}(0, \nu^2/N), \quad (43)$$

$$\text{Im}\delta n_{ij} \sim \mathcal{N}(0, \nu^2/N), \quad (44)$$

$$\nu^2 = \frac{\alpha(1-c)}{2c}, \quad (45)$$

where ν^2/N is the variance of additive coupling noise δn_{ij} . In the case of symmetric dilution, δn_{ij} is symmetric, i.e., $\delta n_{ij} = \overline{\delta n_{ji}}$. On the other hand, in the case of asymmetric dilution, δn_{ij} and δn_{ji} are independent random variables. In the limit of strong dilution, i.e. $c \rightarrow 0$, with α/c kept finite, our system is reduced to a glass oscillator, which corresponds to the Sherrington-Kirkpatrick model of spin glass [21]. Therefore, our theory can cover two types of frustrated systems, the oscillator associative memory system and the glass oscillator system.

In general, the fields h_i^R and h_i^I involve the ORT corresponding to the effective self-feedback [8]. We must eliminate the ORT from these fields. Here, we assume that the local field splits into a "pure" effective local field, $\tilde{h}_i = \tilde{h}_i^R + i\tilde{h}_i^I$, and the ORT, Γs_i :

$$h_i = \tilde{h}_i + \Gamma s_i. \quad (46)$$

We neglect the complex conjugate term of the ORT, which leads to a higher-harmonic term of the coupling function [22]. This can be done in the present model because we use generalized Hebb learning rules (see Appendix). Hence, by substituting Eq. (46) into Eq. (39), we obtain

$$-\frac{d\phi_i}{dt} + \omega_i - \tilde{\Omega} = \sin(\phi_i)\tilde{h}_i^R - \cos(\phi_i)\tilde{h}_i^I, \quad (47)$$

$$\tilde{\Omega} = \Omega - |\Gamma| \sin(\psi), \quad \psi = \text{Arg}(\Gamma), \quad (48)$$

which does not contain the ORT. The quantity $\tilde{\Omega}$ represents the effective frequency of the synchronous oscillators. We can regard $\tilde{\Omega}$ as the renormalized version of Ω , from which the ORT has been removed, so $\tilde{\Omega}$ takes a different value from the observable Ω in general. Thus, $\Omega - \tilde{\Omega}$ represents the contribution of the ORT to the acceleration (deceleration) effect; $\tilde{\Omega}$ is one of the order parameters of our theory. In the analysis that follows, \tilde{h}_i and Γ are obtained in a self-consistent manner (see Appendix).

Let us consider synchronous oscillators in which $\frac{d\phi_i}{d\tau} = 0$ is satisfied in Eq. (47). As a result, the stationary states of the oscillators are satisfied:

$$s_i = \frac{\tilde{h}_i}{|\tilde{h}_i|} \frac{i(\omega_i - \tilde{\Omega}) + \sqrt{|\tilde{h}_i|^2 - (\omega_i - \tilde{\Omega})^2}}{|\tilde{h}_i|}. \quad (49)$$

From Eq. (49), we obtain the following condition for synchronization:

$$|\tilde{h}_i|^2 \geq (\omega_i - \tilde{\Omega})^2. \quad (50)$$

If \tilde{h}_i does not satisfy Eq. (50), ϕ_i continues rotating individually (i.e., desynchronization). This condition corresponds to Eq. (23) for two coupled oscillators. We assume that the microscopic memory effect can be neglected in the $\tau \rightarrow \infty$ limit. In other words, the asymptotic state of the system as $\tau \rightarrow \infty$ is assumed to be independent of the initial conditions at $\tau = 0$. This assumption is exact in non-frustrated systems [17]. Under this assumption, ϕ_i takes the following form:

$$\phi_i = \tilde{\omega}_i \tau + f(\tilde{\omega}_i \tau). \quad (51)$$

where $f(x)$ is a periodic function with period 2π , and $\tilde{\omega}_i$ is the resultant frequency of asynchronous oscillators into which the ORT has been absorbed. $\tilde{\omega}_i$ is given by the following equation:

$$\tilde{\omega}_i = \tilde{\Omega} + (\omega_i - \tilde{\Omega}) \sqrt{1 - \frac{|\tilde{h}_i|^2}{(\omega_i - \tilde{\Omega})^2}}. \quad (52)$$

Applying the SK theory [4] to Eq. (47), we obtain the average of s_i over ω_i :

$$\begin{aligned} \langle s_i \rangle_\omega &= \tilde{h}_i \int_{-\pi/2}^{\pi/2} d\phi g\left(\tilde{\Omega} + |\tilde{h}_i| \sin \phi\right) \cos \phi \exp(i\phi) \\ &+ i\tilde{h}_i \int_0^{\pi/2} d\phi \frac{\cos \phi (1 - \cos \phi)}{\sin^3 \phi} \left\{ g\left(\tilde{\Omega} + \frac{|\tilde{h}_i|}{\sin \phi}\right) - g\left(\emptyset \text{mega} - \frac{|\tilde{h}_i|}{\sin \phi}\right) \right\}. \end{aligned} \quad (53)$$

In this analysis, we focus on the memory retrieval states in which the configuration has appreciable overlap with the condensed pattern ξ^1 ($m^1 \sim O(1)$) and has little overlap with the uncondensed patterns ξ^μ for $\mu > 1$ ($m^\mu \sim O(1/\sqrt{N})$). Under this assumption, we obtain the contribution of the uncondensed patterns using SCSNA (self-consistent signal to noise analysis) [8] and determine \tilde{h}_i in a self-consistent manner (see Appendix). Finally, the equations relating the order parameters $|m^1|$, U , and $\tilde{\Omega}$ are obtained using the self-consistent local field:

$$|m^1| e^{-i\beta_0} = \left\langle \left\langle \tilde{X}(x_1, x_2; \tilde{\Omega}) \right\rangle \right\rangle_{x_1, x_2}, \quad (54)$$

$$U e^{-i\beta_0} = \left\langle \left\langle F_1(x_1, x_2; \tilde{\Omega}) \right\rangle \right\rangle_{x_1, x_2}, \quad (55)$$

where $\langle \langle \dots \rangle \rangle_{x_1, x_2}$ is the Gaussian average over x_1 and x_2 , $\langle \langle \dots \rangle \rangle_{x_1, x_2} = \int \int Dx_1 Dx_2 \dots$. The quantity U corresponds to the susceptibility, which is the measure of the sensitivity to

external fields. Since the present system possesses rotational symmetry with respect to the phase ϕ_i , we can safely set the condensed pattern to $\xi_i^1 = 1$. Now, \tilde{h} , \tilde{X} , F_1 , and Dx_1Dx_2 can be expressed as

$$Dx_1Dx_2 = \frac{dx_1dx_2}{2\pi\rho^2} \exp\left(-\frac{x_1^2+x_2^2}{2\rho^2}\right), \quad (56)$$

$$\rho^2 = \frac{\alpha}{2|1-U|^2} + \nu^2, \quad \nu^2 = \frac{\alpha(1-c)}{2c}, \quad \tilde{h} = |m^1| + x_1 + ix_2, \quad (57)$$

$$\begin{aligned} \tilde{X}(x_1, x_2; \tilde{\Omega}) &= \tilde{h} \int_{-\pi/2}^{\pi/2} d\phi g\left(\tilde{\Omega} + |\tilde{h}| \sin \phi\right) \cos \phi \exp(i\phi) \\ &\quad + i\tilde{h} \int_0^{\pi/2} d\phi \frac{\cos \phi(1 - \cos \phi)}{\sin^3 \phi} \left\{ g\left(\tilde{\Omega} + \frac{|\tilde{h}|}{\sin \phi}\right) - g\left(\tilde{\Omega} - \frac{|\tilde{h}|}{\sin \phi}\right) \right\}, \end{aligned} \quad (58)$$

$$\begin{aligned} F_1(x_1, x_2; \tilde{\Omega}) &= \int_{-\pi/2}^{\pi/2} d\phi \left(g\left(\tilde{\Omega} + |\tilde{h}| \sin \phi\right) + \frac{|\tilde{h}|}{2} \sin \phi g'\left(\tilde{\Omega} + |\tilde{h}| \sin \phi\right) \right) \cos \phi \exp(i\phi) \\ &\quad + i \int_0^{\pi/2} d\phi \frac{\cos \phi(1 - \cos \phi)}{\sin^3 \phi} \left\{ g\left(\tilde{\Omega} + \frac{|\tilde{h}|}{\sin \phi}\right) - g\left(\tilde{\Omega} - \frac{|\tilde{h}|}{\sin \phi}\right) \right\} \\ &\quad + i \frac{|\tilde{h}|}{2} \int_0^{\pi/2} d\phi \frac{\cos \phi(1 - \cos \phi)}{\sin^4 \phi} \left\{ g'\left(\tilde{\Omega} + \frac{|\tilde{h}|}{\sin \phi}\right) + g'\left(\tilde{\Omega} - \frac{|\tilde{h}|}{\sin \phi}\right) \right\} \end{aligned} \quad (59)$$

The terms with the coefficient i in Eqs. (58) and (59) represent the contribution of asynchronous oscillators to the macroscopic behavior. The other terms represent the contribution of the cluster of synchronous oscillators. In the case of the symmetric diluted system, Γ can be expressed as

$$\Gamma e^{-i\beta_0} = \frac{\alpha U}{1-U} + \frac{\alpha(1-c)}{c} U. \quad (60)$$

In the case of the asymmetric diluted system, on the other hand, we have

$$\Gamma e^{-i\beta_0} = \frac{\alpha U}{1-U}. \quad (61)$$

\tilde{h} and $\tilde{\Omega}$ are the renormalized versions of h and Ω , respectively, from which the ORT has been removed, and thus \tilde{h} and $\tilde{\Omega}$ are independent of the ORT. Therefore, the two models we consider have identical order parameter equations, (54) and (55), written using the term of the renormalized quantities \tilde{h} and $\tilde{\Omega}$. From Eq. (48), the difference between the ORTs in Eqs. (60) and (61) leads to a different value for the observable Ω only when $\beta_0 \neq 0$. In this way we are able to clearly separate the effect of the ORT, and therefore, by observing the macroscopic parameter Ω of these two systems, we can analyze the effect of the ORT qualitatively and quantitatively.

The distribution of renormalized resultant frequencies $\tilde{\omega}$ (Eq. (52)) in the memory retrieval state, which is denoted as $\tilde{p}(\tilde{\omega})$, becomes

$$\tilde{p}(\tilde{\omega}) = r\delta(\tilde{\omega} - \tilde{\Omega}) + \int Dx_1 Dx_2 \frac{g\left(\tilde{\Omega} + (\tilde{\omega} - \tilde{\Omega})\sqrt{1 + \frac{|\tilde{h}|^2}{(\tilde{\omega} - \tilde{\Omega})^2}}\right)}{\sqrt{1 + \frac{|\tilde{h}|^2}{(\tilde{\omega} - \tilde{\Omega})^2}}}, \quad (62)$$

$$r = \int Dx_1 Dx_2 |\tilde{h}| \int_{-\pi/2}^{\pi/2} d\phi g\left(\tilde{\Omega} + |\tilde{h}| \sin \phi\right) \cos \phi, \quad (63)$$

The δ -function in Eq. (64) indicates the cluster of oscillators synchronously locked at frequency $\tilde{\Omega}$. The value r is the ratio between the number of synchronous oscillators and the total number of oscillators N . The second term in Eq. (64) represents the distribution of asynchronous oscillators. From the distribution given by Eq. (62), the distribution of observable resultant frequencies $\bar{\omega}$, which is denoted as $p(\bar{\omega})$, becomes

$$p(\bar{\omega}) = \tilde{p}\left(\bar{\omega} - (\Omega - \tilde{\Omega})\right). \quad (64)$$

We now consider the relationships between the present theory and previously proposed theories. If $\beta_0 = 0$ and $g(\omega)$ are symmetric, our theory reduces to the theory proposed by Aonishi et al. [9]:

$$\tilde{X}(x_1, x_2; \tilde{\Omega}) = \tilde{h} \int_{-1}^1 dx g\left(|\tilde{h}|x\right) \sqrt{1 - x^2}, \quad (65)$$

$$F_1(x_1, x_2; \tilde{\Omega}) = \int_{-1}^1 dx \left(g\left(|\tilde{h}|x\right) + \frac{|\tilde{h}|}{2} x g'\left(|\tilde{h}|x\right)\right) \sqrt{1 - x^2}. \quad (66)$$

where $\tilde{\Omega} = \Omega = 0$, since F_1 and U are real numbers. If $g(\omega) = \delta(\omega)$, $\beta_0 = 0$, and $c_{ij} = c_{ji}$, where the present model reduces to an XY-spin system, we obtain

$$\tilde{X} = \frac{\tilde{h}}{|\tilde{h}|}, \quad F_1 = \frac{1}{2|\tilde{h}|}, \quad p(\bar{\omega}) = \delta(\bar{\omega}), \quad (67)$$

which coincide with the replica theory of Cook [19] and SCSNA [23]. In addition, in the

uniform-system limit, $\alpha \rightarrow 0$, our theory reproduces the SK theory [4]:

$$\begin{aligned} |m^1|e^{-i\beta_0} &= |m^1| \int_{-\pi/2}^{\pi/2} d\phi g\left(\tilde{\Omega} + |m^1| \sin \phi\right) \cos \phi \exp(i\phi) \\ &+ i|m^1| \int_0^{\pi/2} d\phi \frac{\cos \phi(1 - \cos \phi)}{\sin^3 \phi} \left\{ g\left(\tilde{\Omega} + \frac{|m^1|}{\sin \phi}\right) - g\left(\tilde{\Omega} - \frac{|m^1|}{\sin \phi}\right) \right\}, \end{aligned} \quad (68)$$

$$p(\bar{\omega}) = r\delta(\bar{\omega} - \Omega) + \frac{g\left(\Omega + (\bar{\omega} - \Omega)\sqrt{1 + \frac{|m^1|^2}{(\bar{\omega} - \Omega)^2}}\right)}{\sqrt{1 + \frac{|m^1|^2}{(\bar{\omega} - \Omega)^2}}}, \quad (69)$$

$$r = |m^1| \int_{-\pi/2}^{\pi/2} d\phi g\left(\Omega + |m^1| \sin \phi\right) \cos \phi, \quad (70)$$

$$\tilde{\Omega} = \Omega. \quad (71)$$

In the limit $N \rightarrow \infty$, models with random dilution are equivalent to models with additive coupling noise [11, 12, 13]. In the limit $c \rightarrow 0$ with α/c kept finite, our system is equivalent to a glass oscillator system with complex interaction. The equations relating the order parameters $|m^1|$ and $\tilde{\Omega}$ are

$$|m^1|e^{-i\beta_0} = \left\langle \left\langle \tilde{X}(x_1, x_2; \tilde{\Omega}) \right\rangle \right\rangle_{x_1, x_2}, \quad (72)$$

$$Dx_1 Dx_2 = \frac{dx_1 dx_2}{2\pi\nu^2} \exp\left(-\frac{x_1^2 + x_2^2}{2\rho^2}\right), \quad (73)$$

$$\rho^2 = \nu^2 = \frac{\alpha}{2c}, \quad \tilde{h} = |m^1| + x_1 + ix_2, \quad (74)$$

$$\begin{aligned} \tilde{X}(x_1, x_2; \tilde{\Omega}) &= \tilde{h} \int_{-\pi/2}^{\pi/2} d\phi g\left(\tilde{\Omega} + |\tilde{h}| \sin \phi\right) \cos \phi \exp(i\phi) \\ &+ i\tilde{h} \int_0^{\pi/2} d\phi \frac{\cos \phi(1 - \cos \phi)}{\sin^3 \phi} \left\{ g\left(\tilde{\Omega} + \frac{|\tilde{h}|}{\sin \phi}\right) - g\left(\tilde{\Omega} - \frac{|\tilde{h}|}{\sin \phi}\right) \right\}. \end{aligned} \quad (75)$$

The above order parameter equations do not contain susceptibility U .

VI. SIMULATION

A. Acceleration (deceleration) effect

In the numerical simulations we now discuss, we set the distribution of natural frequencies as

$$g(\omega) = (2\pi\sigma^2)^{-1/2} \exp(-\omega^2/2\sigma^2), \quad (76)$$

and we used the Euler scheme with a time increment of 0.1, which gave a sufficiently good approximation compared to that of smaller time increments. The resultant frequencies $\bar{\omega}_i$ were calculated using a long time average of $d\phi_i/d\tau$. The acceleration (deceleration) effect was defined as follows: one large cluster of oscillators are synchronously locked at a faster (slower) speed than the mean natural rotation speed of all the oscillators.

First, we set $\beta_0 = \pi/20$, $c = 1.0$ (i.e., no dilution), and $\sigma = 0.2$. Figure 3(a) shows $|m^1|$ as a function of α , and Fig. 3(b) shows Ω and $\tilde{\Omega}$ as functions of α in the memory states. The solid curves were obtained theoretically, and the data points with error bars represent results obtained by numerical simulation. As previously discussed, the ORT was removed from $\tilde{\Omega}$, so the value of $\tilde{\Omega}$ differed from that of the observable Ω . The gap between Ω and $\tilde{\Omega}$ in Figure 3(b) is in proportion to the absolute value of the ORT, as described in Eq. (48). Thus, increasing loading rate α tended to accelerate all of the oscillators due to the effect of the ORT. Figure 3(c) shows Ω as a function of α in the spurious memory states, where Ω corresponds to the maximum point of a histogram of $\bar{\omega}_i$. Compared to Fig. 3(b), the profile of the curve in Fig. 3(c) is different from that of the memory states. This is a very important phenomenon in the context of engineering because, from the results shown in Figs. 3(b) and (c), we can determine if the recall process is successful or not by estimating the difference in the rotation speeds of the oscillators. Figure 3(d) shows histograms of the resultant frequencies $\bar{\omega}_i$ in the memory and spurious memory states, which were obtained by numerical simulation ($\alpha = 0.022$). In this graph, we shifted the center of the peak to 0 and superimposed the solid curves obtained theoretically for the memory states. The theoretical memory-state results are in good agreement with the simulation ones.

Next, to make confirm that the acceleration (deceleration) effect is caused by the ORT, we analyzed oscillator associative memory models involving two types of diluted couplings. We set $\sigma = 0.2$, $\beta_0 = \pi/20$, and $c = 0.5$. Figure 4(a) shows Ω as a function of α in the memory retrieval states; the solid curves were obtained theoretically, and the data points with error bars represent results obtained by numerical simulation. It shows that the oscillator rotated faster in the symmetric diluted system than in the asymmetric one. As previously discussed, $\tilde{\Omega}$ in Fig. 4(a), which represents the effective frequency of synchronous oscillators, does not depend on the type of dilution, while the observed Ω strongly depended on it. This dependence was due to the existence of the ORT. If local field h does not contain the ORT [10], plots obtained from numerical simulations of both models should fit the curve

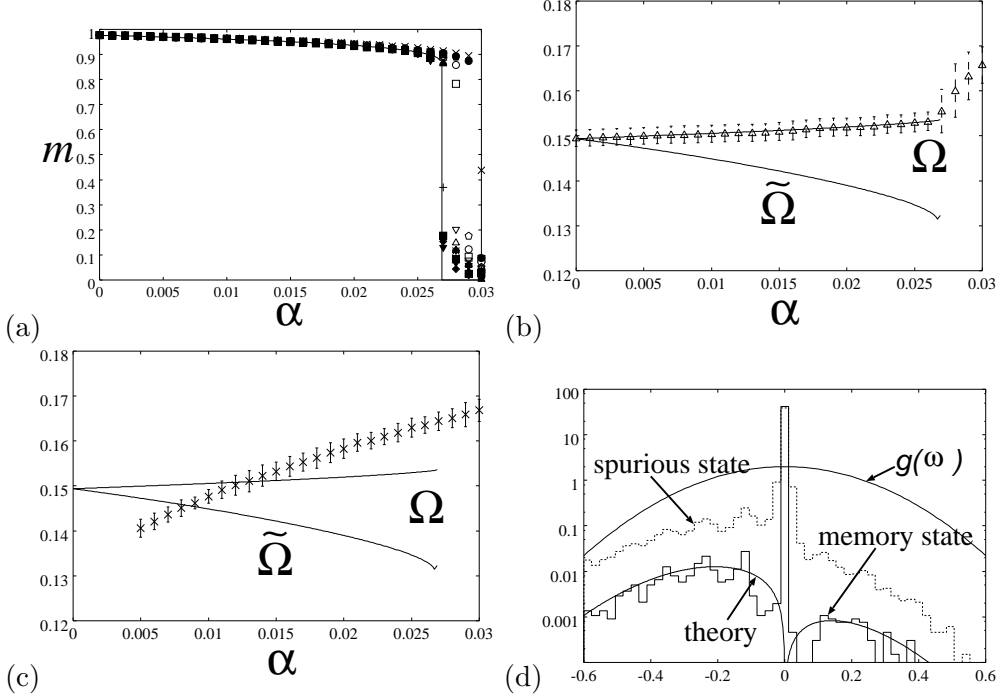


FIG. 3: Simulated and theoretical results when $\beta_0 = \pi/20$, $\sigma = 0.2$, $c = 1.0$, $N = 20000$. Solid curves were theoretically obtained; plots were obtained by numerical simulation. (a) $|m^1|$ as a function of α . (b) Ω as a function of α in memory states. (c) Ω as a function of α in spurious memory states. To compare Ω in spurious memory states with that in the memory states, we superimposed theoretical Ω in the memory states. (d) Distribution of resultant frequencies $\bar{\omega}_i$ in memory and spurious memory states. $\alpha = 0.022$. The center of the delta peak shifted to 0.

of $\tilde{\Omega}$. Therefore, the dependence of the observed Ω on the type of dilution is strong evidence for the existence of the ORT in the present system. In this figure, we shifted the numerical values of Ω at $\alpha = 0$ (in the computer simulation) to their corresponding theoretical values at $\alpha = 0$ in order to cancel fluctuations in the mean value of $g(\omega)$ caused by the finite-size effect.

Figures 4(b) and (c) show the distributions of the resultant frequencies for the symmetric and asymmetric dilution systems, respectively. The theoretical results (solid curve) are in good agreement with the simulated one (histogram). From the results given in Figs. 4(b) and (c), the distribution of the resultant frequencies for the symmetric diluted system is identical to that for the asymmetric diluted system, except for differences in positions caused by the ORT. We thus conclude that the mean field, \tilde{h} , of the symmetric diluted

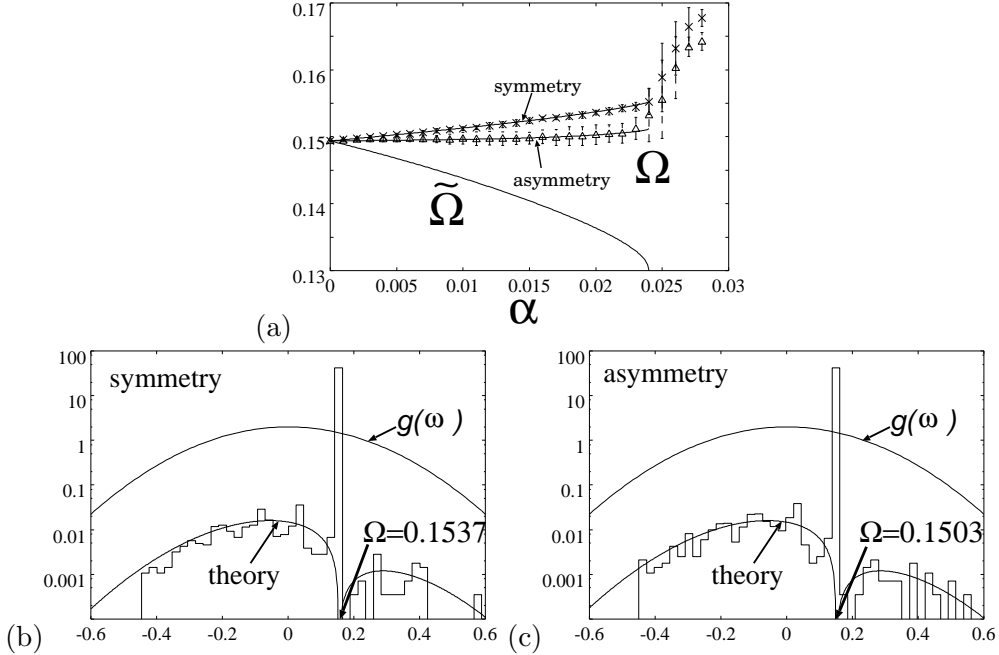


FIG. 4: Difference between symmetric and asymmetric dilution systems; $N = 10,000$, $\sigma = 0.2$, $\beta_0 = \pi/20$, and $c = 0.5$. (a) Ω as a function of α . (b) Distribution of resultant frequencies for symmetric dilution system ($\alpha = 0.02$). (c) Distribution of resultant frequencies for asymmetric dilution system ($\alpha = 0.02$).

system is identical to that of the asymmetric diluted system, since \tilde{h} reflects the distribution of resultant frequencies, as represented by Eq. (64). Figures 5(a) and (b) show $|m^1|$ as a function of α for the symmetric and asymmetric diluted systems, respectively. The solid curves were obtained theoretically, and the data plots represent the results obtained from numerical simulations. As the figures show, the critical memory capacities of the two models are equal.

Consequently, symmetric and asymmetric diluted systems have the same macroscopic properties, with the exception of the acceleration (deceleration) effect caused by the ORT. The quantity of the ORT depends on the type of dilution, and this dependence leads to a difference in the rotation speeds of the oscillators for the two cases, as shown in Fig. 4(a).

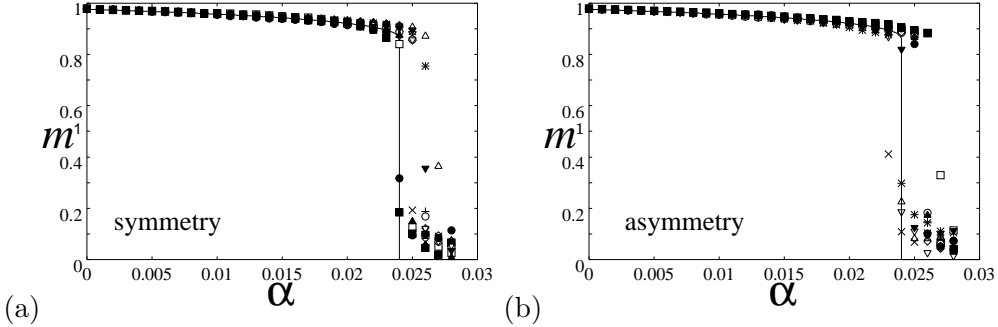


FIG. 5: $|m^1|$ as a function of α . Solid curves were obtained theoretically, and data points were obtained by numerical simulation; $N = 10,000$, $\sigma = 0.2$, $\beta_0 = \pi/20$, and $c = 0.5$. (a) Symmetric dilution system. (b) Asymmetric dilution system.

B. Glass oscillators

In the numerical simulations described here, we used a random symmetric coupling system instead of the symmetric diluted system. We randomly chose those couplings using two probability functions: $J_{ij} \cos(\beta_{ij}) \sim \mathcal{N}(1/N, \nu^2/N)$ and $J_{ij} \sin(\beta_{ij}) \sim \mathcal{N}(1/N, \nu^2/N)$, where we restrict mutual couplings to symmetric ones, $J_{ij} \exp(i\beta_{ij}) = J_{ji} \exp(-i\beta_{ji})$ and set $\beta_0 = 0$. Figure 6 shows a phase diagram in the $(|m^1|, \sigma, \nu)$ space, which was obtained by numerically solving the order parameter equation (72). A cross-section of this curved surface at $\nu = 0$ is equal to a result of the SK theory [4]. Figures 7(a), (b), (c), and (d) display $|m^1|$ as a function of σ for various values of ν ; the solid curves were obtained theoretically, and the data points show results obtained by numerical simulation. Figures 8(a) and (b) show the distributions of the resultant frequencies $\bar{\omega}_i$ in the ferromagnetic state. As Figs. 7 and 8 reveal, when $|m^1|$ was small, the theoretical curves did not fit the simulation results very well. We surmise that the gap between the simulation results and theoretical results might have been caused by the ergodicity breaking with the ultrametric structure of the glass states; this breaking is related to replica-symmetry breaking [24, 25, 26]. Unfortunately, our theory does not capture the ultrametric structure of the glass states; it focuses only on one of the pure states in the phase space. In the next section, we will explain the glass phase in detail.

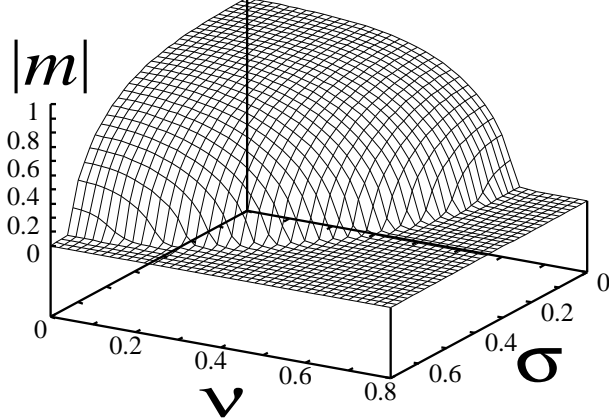


FIG. 6: Phase diagram in $(|m^1|, \sigma, \nu)$ space ($\beta_0 = 0$) of spin glass model.

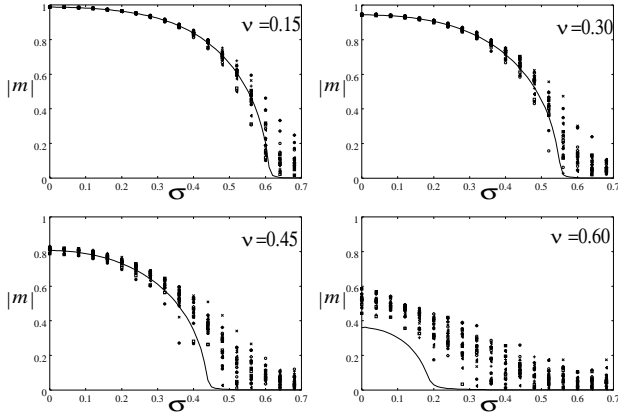


FIG. 7: $|m^1|$ as a function of σ (solid curves were theoretically obtained; plots were obtained by numerical simulation). $\beta_0 = 0$, $N = 2000$.

C. Properties of spurious memory state

Here, we examine the properties of spurious memory states. In the following analyses, we set $c = 0.5$, $\alpha = 0.025$, $\sigma = 0.16$, and $\beta_0 = 0$.

Figures 9 (a), (a'), (b), and (b') show histograms of resultant frequencies $\bar{\omega}_i$ in memory states and superimpose histograms of $\bar{\omega}_i$ in spurious memory states. Figures 9 (b) and (b') show in detail the structures of the sharp peaks at the center $\bar{\omega} = 0$ in Figs. 9 (a) and (a'), respectively. Figures 9 (a) and (b) correspond to the cases of asymmetric diluted systems, and Figs. 9 (a') and (b') correspond to the cases of symmetric diluted systems.

As shown in Figs. 9 (a) and (a'), in memory retrieval states, a single delta-peak exists at $\bar{\omega} = 0$, which corresponds to a large cluster of synchronous oscillators, and asynchronous

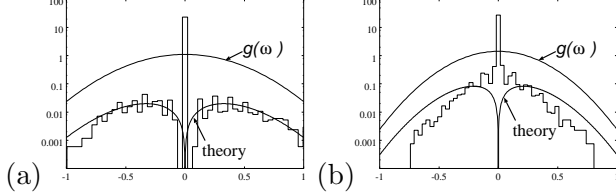


FIG. 8: Distribution of resultant frequencies $\bar{\omega}_i$ in ferromagnetic states. (a) $\nu = 0.15$, $\sigma = 0.36$, $\beta_0 = 0$. (b) $\nu = 0.45$, $\sigma = 0.28$, $\beta_0 = 0$.

oscillators are symmetrically distributed around the delta-peak.

On the other hand, as shown in Figs. 9 (a) and (a'), in spurious memory states, a sharp peak exists at $\bar{\omega} = 0$. As Figs. 9 (b) and (b') reveal, the peak of the spurious memory states at $\bar{\omega} = 0$ is gentler than that of the memory retrieval states. These gentle peak indicates that the entrainment in the glass phase is weaker than that in the ferromagnetic phase. This phenomenon corresponds to the so-called *quasi-entrainment* observed in the glass oscillator system [14]. As shown in Figs. 9 (a) and (a'), the degree of asynchronous oscillators in the spurious memory states is larger than that in the memory states. As the results obtained from analyses of the system in the memory and spurious memory states reveal, we can determine if the recall process is successful or not by using information about the degrees of the synchronous oscillators. Note that it is difficult for attractor-type networks used to solve optimization problems to detect being trapped in a meta-stable state during the relaxation process. This new finding indicates that a class of non-equilibrium systems can potentially be used to address the detection of meta-stable states.

Figures 10(a), (b), (c), and (d) show histograms of the absolute value of local field $|h|$ in the memory and spurious memory states. Since the present system possesses rotational symmetry with respect to the phase ϕ_i , we can safely define the condensed pattern as $\xi_i^1 = 1$; i.e., the gauge transformation can be performed on variables of the condensed pattern. After the gauge transformation, if the system is in the memory states, the histogram of local field h is given as a two-dimensional isotropic Gaussian at $h = m^1$ in the complex plane. However, the histogram of h in the spurious memory state takes a "volcanic" form around $h = 0$ in the complex plane. Such a histogram form for the local field was also observed in the glass oscillator system [14]. It is well-known that in equilibrium systems, the spin glass states have an ultrametric tree structure [24, 26]. This structure of the spin glass states can be expressed using the replica symmetric breaking scheme in replica theory, which is based on

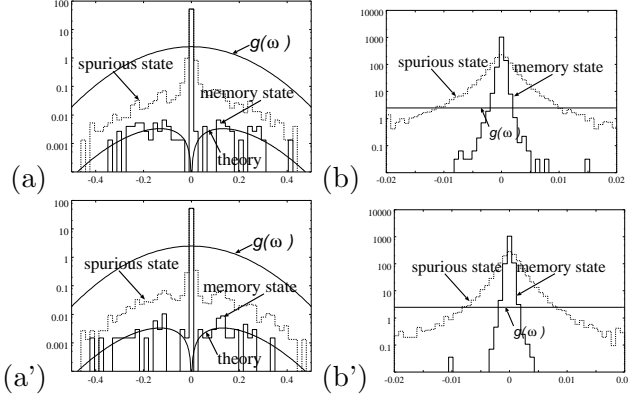


FIG. 9: Distribution of resultant frequencies $\bar{\omega}_i$ in memory and spurious memory states. $c = 0.5$, $\alpha = 0.025$, $\sigma = 0.16$, and $\beta_0 = 0$; (b) and (b') show in detail the structure of the sharp peaks at the center $\bar{\omega} = 0$ of 9 in (a) and (a'), respectively. (a) and (b) asymmetry dilution; (a') and (b') symmetry dilution.

a multi-cascade Gaussian process for generating the local field [25]. We surmise that even in the non-equilibrium systems proposed here, a multi-cascade Gaussian process in the glass states results in a non-Gaussian distribution of the local field, as shown in Figs. 10(a), (b), (c), and (d).

As mentioned above, our theory does not capture the ultrametric structure of the glass states; it focuses only on one of the pure states in the phase space. This is because SCSNA is based on the Gaussian ansatz for the local field, which is deeply related to replica symmetric approximation in replica theory [8]. Even in the spurious memory state, SCSNA and replica theory under replica symmetric approximation give the probability distribution of the local field as a single Gaussian at $h = 0$ in the complex plane. However, no one has been able to explain the ultrametric structure of the glass states in the SCSNA framework. Therefore, to properly analyze the systems in spurious states (glass states), we need to extend the present theory to a more general theory, one that treats an ultrametric structure.

VII. CONCLUSION

We have proposed a curved isochron clock (CIC) based on the radial isochron clock that provides a clean example of the acceleration (deceleration) effect. By analyzing two-body system of coupled CICs, we showed that an unbalanced mutual interaction caused by curved

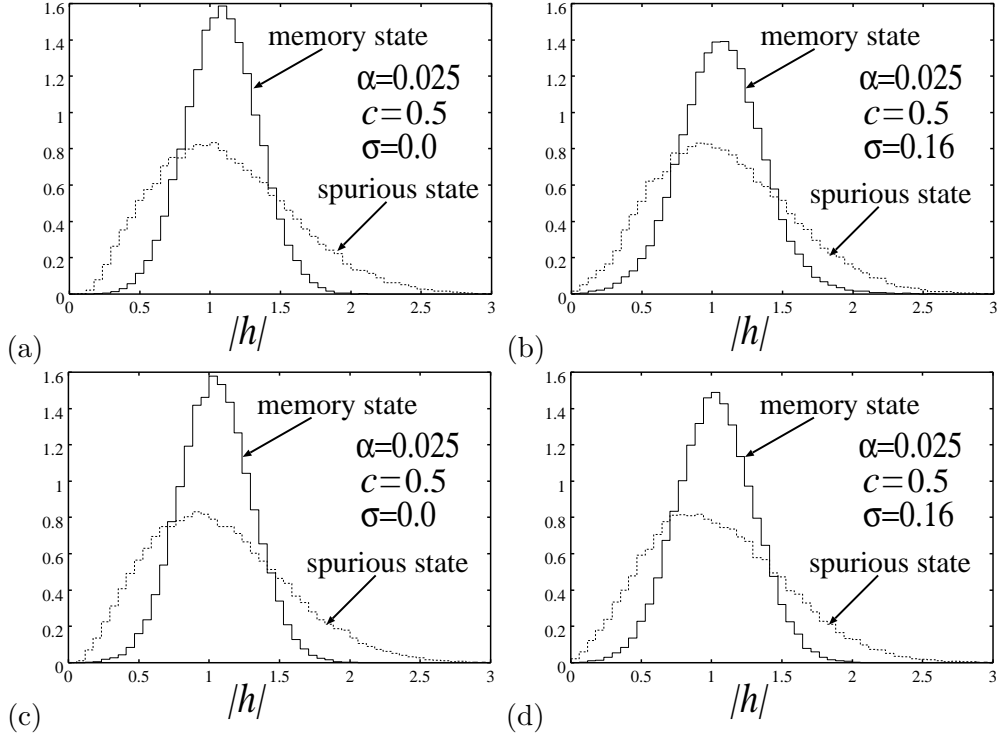


FIG. 10: Distribution of local field in memory and spurious memory states. $\beta_0 = 0$. (a) and (b) show results of numerical simulation for systems with symmetry dilution; (c) and (d) show those of systems with asymmetry dilution.

isochron sets is the minimum mechanism needed for generating the acceleration (deceleration) effect in coupled oscillator systems. From this we determined that the Sakaguchi and Kuramoto (SK) model, which is a mean field model of coupled oscillators without frustration, has such a mechanism. To study frustrated coupled oscillator systems, we extend the SK model to two oscillator associative memory models, one with symmetric and one with asymmetric dilution of coupling, which also have the minimum mechanism for the acceleration (deceleration) effect. We theoretically showed that the *Onsager reaction term* (ORT), which is unique to frustrated systems, plays an important role in the acceleration (deceleration) effect. Comparing the two models, we extracted the effect of the ORT only to the rotation speed of the oscillators.

The acceleration (deceleration) effect caused by the ORT is peculiar to non-equilibrium systems, since this effect only occurs when $\beta_0 \neq 0$. There has been fundamental disagreement regarding the existence of the ORT in a typical system corresponding to our model with $\beta_0 = 0$ and a symmetric $g(\omega)$ [9, 10]. From the results of this work we conclude that even if

$\beta_0 = 0$ and $g(\omega)$ is symmetric, the ORT exists in the bare local field given by Eq. (40). In this case, the effect of the ORT is not detectable because it cancels out of Eq. (47).

As the results illustrated in Figs 5(a) and (b) reveal, the critical memory capacity of the asymmetric diluted systems obtained from numerical simulation is slightly smaller than that of the symmetric ones, because asymmetric dilution breaks the detailed balance of the system, which weakens the stability of the memory states. There is yet no theory to rigorously treat a system with asymmetric interaction. Most theoretical studies of asymmetric systems are based on the naive assumption that there are such steady states as equilibrium states of symmetric systems [13].

In the field of neuroscience, a growing number of researchers are becoming interested in the synchrony of oscillatory neural activities because physiological evidence of their existence has been obtained in the visual cortex of a cat [27, 28]. Much experimental and theoretical research has been done on the functional role of synchronization. One of the more interesting hypotheses is called *synchronized population coding*, which was proposed by Phillips and Singer [29]. However, its validity is highly controversial. In this paper, we numerically showed the possibility of determining if the recall process was successful or not by using information about the synchrony/asynchrony. If we consider information processing in brain systems, the solvable *toy* model presented in this paper may be a good candidate for showing the validity of a synchronized population coding in the brain. According to anatomical and physiological data, the olfactory system can be considered as an associative memory with oscillatory behavior. There is one particularly interesting finding related to our studies. Freeman and Sharda demonstrated chaotic behavior of olfactory neural systems in response to unknown odors [30]. We suspect that this chaotic behavior is related to the asynchronous behavior of our systems in spurious memory states. Thus, the present analysis should strongly affect the debate on the functional role of synchrony.

Appendix: Derivation of order parameter equations

Assuming a pure effective local field, \tilde{h}_i , in Eq. (46), we performed renormalization of the local field expressed in Eq. (47). The quantity $\tilde{\Omega}$ in Eq. (47) is the renormalized version of Ω , from which the ORT has been removed. Thus, \tilde{h}_i is independent of any macroscopic configuration of unit i . In this way, by performing renormalization of the local field, we can

reduce large population systems to one-body problems. Under the assumption formalized in Eq. (46), the distribution of s_i , which is denoted as $n(\phi_i; \tilde{h}_i, \tilde{\Omega})$, can be formally derived using SK theory.

In the framework of the SK theory, we can split the distribution of s_i into a synchronized part and a desynchronized part as $n(\phi_i; \tilde{h}_i, \tilde{\Omega}) = n_s(\phi_i; \tilde{h}_i, \tilde{\Omega}) + n_{ds}(\phi_i; \tilde{h}_i, \tilde{\Omega})$. $n_s(\phi_i; \tilde{h}_i, \tilde{\Omega})$ represents the distribution of synchronous oscillators and $n_{ds}(\phi_i; \tilde{h}_i, \tilde{\Omega})$ denotes the distribution of asynchronous ones. First, we derive $n_s(\phi_i; \tilde{h}_i, \tilde{\Omega})$ from Eq. (47) ($\frac{d\phi_i}{d\tau} = 0$) as follows,

$$\begin{aligned} n_s(\phi_i; \tilde{h}_i, \tilde{\Omega}) &= \int d\omega_i g(\omega_i) \delta \left(\omega_i - \tilde{\Omega} - \sin(\phi_i) \tilde{h}_i^R + \cos(\phi_i) \tilde{h}_i^I \right) \\ &= g \left(\tilde{\Omega} + \tilde{h}_i^R \sin(\phi_i) - \tilde{h}_i^I \cos(\phi_i) \right) \left(\tilde{h}_i^R \cos(\phi_i) + \tilde{h}_i^I \sin(\phi_i) \right), \\ &\quad -\frac{\pi}{2} + \tan^{-1} \frac{\tilde{h}_i^I}{\tilde{h}_i^R} \leq \phi_i \leq \frac{\pi}{2} + \tan^{-1} \frac{\tilde{h}_i^I}{\tilde{h}_i^R}. \end{aligned} \quad (77)$$

Next, we consider $n_{ds}(\phi_i; \tilde{h}_i, \tilde{\Omega}, \omega_i)$ which represents a conditional probability distribution of $n_{ds}(\phi_i; \tilde{h}_i, \tilde{\Omega})$. $n_{ds}(\phi_i; \tilde{h}_i, \tilde{\Omega}, \omega_i)$ is governed by the following Liouville equation,

$$\frac{\partial}{\partial \tau} n_{ds}(\phi_i; \tilde{h}_i, \tilde{\Omega}, \omega_i) = -\frac{\partial}{\partial \phi_i} \left((\omega_i - \tilde{\Omega} - \sin(\phi_i) \tilde{h}_i^R + \cos(\phi_i) \tilde{h}_i^I) n_{ds}(\phi_i; \tilde{h}_i, \tilde{\Omega}, \omega_i) \right). \quad (78)$$

In the limit that $\tau \rightarrow \infty$, the stationary distribution becomes

$$\begin{aligned} n_{ds}(\phi_i; \tilde{h}_i, \tilde{\Omega}, \omega_i) &= C(\omega_i - \tilde{\Omega} - \sin(\phi_i) \tilde{h}_i^R + \cos(\phi_i) \tilde{h}_i^I)^{-1} \\ C &= 1 / \int_0^{2\pi} d\phi_i (\omega_i - \tilde{\Omega} - \sin(\phi_i) \tilde{h}_i^R + \cos(\phi_i) \tilde{h}_i^I)^{-1} \\ &= \frac{\omega_i - \tilde{\Omega}}{2\pi} \sqrt{1 - \frac{|\tilde{h}_i|^2}{(\omega_i - \tilde{\Omega})^2}}. \end{aligned} \quad (79)$$

Then, $n_{ds}(\phi_i; \tilde{h}_i, \tilde{\Omega})$ is expressed as

$$n_{ds}(\phi_i; \tilde{h}_i, \tilde{\Omega}) = \frac{1}{2\pi} \int_{|\omega_i - \tilde{\Omega}| > |\tilde{h}_i|} d\omega_i g(\omega_i) \frac{(\omega_i - \tilde{\Omega}) \sqrt{1 - \frac{|\tilde{h}_i|^2}{(\omega_i - \tilde{\Omega})^2}}}{\omega_i - \tilde{\Omega} - \sin(\phi_i) \tilde{h}_i^R + \cos(\phi_i) \tilde{h}_i^I}. \quad (80)$$

Averaging s_i over ω_i , that is, $\langle s_i \rangle_{\omega_i} = \int d\phi_i n(\phi_i; \tilde{h}_i, \tilde{\Omega}) \exp(i\phi_i)$, we obtain the following

equation,

$$\begin{aligned}
\left\langle s_i(\tilde{h}_i) \right\rangle_{\omega_i} &= \tilde{h}_i \int_{-\pi/2}^{\pi/2} d\phi_i g\left(\tilde{\Omega} + |\tilde{h}_i| \sin \phi_i\right) \cos \phi_i \exp(i\phi_i) \\
&+ i \frac{\tilde{h}_i}{|\tilde{h}_i|} \int_{|\omega_i - \tilde{\Omega}| > |\tilde{h}_i|} d\omega_i g(\omega_i)(\omega_i - \tilde{\Omega}) \left(1 - \sqrt{1 - \frac{|\tilde{h}_i|^2}{(\omega_i - \tilde{\Omega})^2}}\right) \\
&= \tilde{h}_i \int_{-\pi/2}^{\pi/2} d\phi_i g\left(\tilde{\Omega} + |\tilde{h}_i| \sin \phi_i\right) \cos \phi_i \exp(i\phi_i) \\
&+ i \tilde{h}_i \int_0^{\pi/2} d\phi_i \frac{\cos \phi_i (1 - \cos \phi_i)}{\sin^3 \phi_i} \left\{ g\left(\tilde{\Omega} + \frac{|\tilde{h}_i|}{\sin \phi_i}\right) - g\left(\tilde{\Omega} - \frac{|\tilde{h}_i|}{\sin \phi_i}\right) \right\}. \quad (81)
\end{aligned}$$

Note that if $g(\tilde{\Omega} + x) = g(\tilde{\Omega} - x)$, we can neglect the effect of asynchronous oscillators. When $g(x) = \delta(x)$ and $\beta_0 = 0$, we obtain

$$\left\langle s_i(\tilde{h}_i) \right\rangle_{\omega} = \frac{\tilde{h}_i}{|\tilde{h}_i|}. \quad (82)$$

Next, we estimate \tilde{h}_i in the framework of SCSNA. In this analysis, we focus on the memory retrieval states, in which the configuration has appreciable overlap with the condensed pattern ξ^1 ($m^1 \sim O(1)$) and has little overlap with the uncondensed patterns ξ^μ for $\mu > 1$ ($m^\mu \sim O(1/\sqrt{N})$). Under this assumption, we estimate the contribution of the uncondensed patterns using SCSNA [8] and determine \tilde{h}_i in a self-consistent manner. In the first step of SCSNA, we split local field h_i into a signal part (the first term), a cross-talk noise part (the second term), and a coupling noise part (the third term):

$$h_i e^{-i\beta_0} = \xi_i^1 m^1 + \sum_{\mu > 1} \xi_i^\mu m^\mu + \sum_{j(\neq i)}^N \delta n_{ij} s_j - \alpha s_i. \quad (83)$$

In the next step, we split the cross-talk noise (the second term) and the coupling noise (the third term), respectively, into the Gaussian random variable and the ORT. Equation (39) implies that s_i is a function of local field h_i , natural frequency $\omega_i - \Omega$, and time τ ; that is,

$$s_i = X(h_i, \omega_i - \Omega, \tau). \quad (84)$$

Note that s_i is not a function of renormalized \tilde{h}_i and $\tilde{\Omega}$; instead, it is a function of the bare h_i and Ω in Eq. (39). We can properly evaluate the ORT with this careful treatment. Here, we assume that the microscopic memory effect can be neglected in the $\tau \rightarrow \infty$ limit. In

general, $X(h_i, \omega_i - \Omega, \tau)$ is not regular. As such, a variation in X due to a small perturbation in local field h denoted dh is satisfied

$$dX = u(h, \omega - \Omega, \tau)dh + v(h, \omega - \Omega, \tau)d\bar{h}. \quad (85)$$

Therefore, $m^\mu \sim O(1/\sqrt{N})$, $\mu \geq 2$ is expressed as

$$\begin{aligned} m^\mu &= \frac{1}{N} \sum_i \bar{\xi}_i^\mu X(h_i, \omega_i - \Omega, \tau) \\ &= \frac{1}{N} \sum_i \bar{\xi}_i^\mu X_i^{(\mu)} + U_1 m^\mu e^{i\beta_0} + V_1 \bar{m}^\mu e^{-i\beta_0}, \end{aligned} \quad (86)$$

$$U_1 = \frac{1}{N} \sum_i \bar{\xi}_i^\mu \xi_i^\mu u(h_i^{(\mu)}, \omega_i - \Omega, \tau), \quad (87)$$

$$V_1 = \frac{1}{N} \sum_i \bar{\xi}_i^\mu \bar{\xi}_i^\mu v(h_i^{(\mu)}, \omega_i - \Omega, \tau), \quad (88)$$

where

$$\begin{aligned} X_i^{(\mu)} &= X\left(h_i^{(\mu)}, \omega_i - \Omega, \tau\right), \\ h_i^{(\mu)} e^{-i\beta_0} &= \sum_{\nu(\neq\mu)} \xi_i^\nu m^\nu + \sum_{j(\neq i)}^N \delta n_{ij} s_j - \alpha s_i. \end{aligned} \quad (89)$$

Note that $X_i^{(\mu)}$ is uncorrelated with ξ_i^μ . We can neglect the complex conjugate term V_1 , which leads to a higher-harmonic term of the coupling function [22], since $E\left[\bar{\xi}_i^\mu \bar{\xi}_i^\mu\right] = 0$.

From Eq. (86), we obtain

$$m^\mu = \frac{1}{N(1 - e^{i\beta_0} U_1)} \sum_j \bar{\xi}_j^\mu X_j^{(\mu)}. \quad (90)$$

Substituting Eq. (90) into the cross-talk noise of Eq. (83), in the limit $N \rightarrow \infty$, we can split the cross-talk noise into the Gaussian random variable and the ORT:

$$\sum_{\mu=2}^{\alpha N} \xi_i^\mu m^\mu = z_i^A + \frac{\alpha}{1 - e^{i\beta_0} U} s_i, \quad (91)$$

$$z_i^A = \frac{1}{N(1 - e^{i\beta_0} U)} \sum_{\mu=1}^{\alpha N} \sum_{j(\neq i)} \xi_i^\mu \bar{\xi}_j^\mu X_j^{(\mu)}, \quad (92)$$

$$U = \frac{1}{N} \sum_i u(h_i, \omega_i - \Omega, \tau), \quad (93)$$

Next, we split the coupling noise term of Eq. (83) into the Gaussian random variable and the ORT.

$$\begin{aligned} \sum_{j \neq i}^N \delta n_{ij} s_j &= \sum_{j(\neq i)}^N \delta n_{ij} X_j^{(i)} \\ &+ s_i e^{i\beta_0} U_2 + \bar{s}_i e^{-i\beta_0} V_2, \end{aligned} \quad (94)$$

$$U_2 = \frac{1}{N} \sum_{j(\neq i)}^N \delta n_{ij} \delta n_{ji} u(h_j^{(i)}, \omega_j - \Omega, \tau), \quad (95)$$

$$V_2 = \frac{1}{N} \sum_{j(\neq i)}^N \delta n_{ij} \bar{\delta n_{ji}} v(h_j^{(i)}, \omega_j - \Omega, \tau), \quad (96)$$

where

$$\begin{aligned} X_i^{(j)} &= X \left(h_i^{(j)}, \omega_i - \Omega, \tau \right), \\ h_i^{(j)} e^{-i\beta_0} &= \sum_{\nu} \xi_{\nu}^{\nu} m^{\nu} + \sum_{k(\neq i, j)}^N \delta n_{ik} s_k - \alpha s_i, \end{aligned} \quad (97)$$

Note that $X_i^{(j)}$ is uncorrelated with δn_{ij} . We can also neglect the complex conjugate term V_2 , which leads to a higher-harmonic term of the coupling function [22], since $E[\delta n_{ij} \bar{\delta n_{ji}}] = 0$. For the symmetric diluted system, $E[\delta n_{ij} \delta n_{ji}] = \frac{2\nu^2}{N}$, so, in the limit $N \rightarrow \infty$, we can split the coupling noise term of Eq. (83) into the Gaussian random variable and the ORT:

$$\sum_{j=1}^N \delta n_{ij} s_j = z_i^G + 2\nu^2 e^{i\beta_0} U s_i, \quad (98)$$

$$z_i^G = \sum_{j(\neq i)}^N \delta n_{ij} X_j^{(i)} \quad (99)$$

$$U = \frac{1}{N} \sum_j^N u(h_j, \omega_j - \Omega, \tau), \quad (100)$$

For the asymmetric diluted system, we can neglect the ORT in the coupling noise term:

$$\sum_{j=1}^N \delta n_{ij} s_j = z_i^G, \quad (101)$$

$$z_i^G = \sum_{j(\neq i)}^N \delta n_{ij} X_j^{(i)}, \quad (102)$$

since $E[\delta n_{ij} \delta n_{ji}] = 0$.

From these manipulations, local field h_i is given by

$$h_i e^{-i\beta_0} = \xi_i^1 m^1 + z_i^A + z_i^G + \Gamma s_i \quad (103)$$

$$\Gamma = \frac{\alpha e^{i\beta_0} U}{1 - e^{i\beta_0} U} + 2\nu^2 e^{i\beta_0} U \quad (\text{symmetric}), \quad (104)$$

$$\Gamma = \frac{\alpha e^{i\beta_0} U}{1 - e^{i\beta_0} U} \quad (\text{asymmetric}), \quad (105)$$

where $z_i^A + z_i^G$ is a random variable of an isotropic 2-dimensional Gaussian that satisfies

$$\begin{aligned} E [\text{Re}[z_i^A + z_i^G]^2] &= E [\text{Im}[z_i^A + z_i^G]^2] \\ &= \frac{\alpha}{2|1 - e^{i\beta_0} U|^2} + \nu^2, \\ E [\text{Re}[z_i^A + z_i^G] \text{Im}[z_i^A + z_i^G]] &= 0, \end{aligned}$$

In the final step of SCSNA, we determine a pure effective local field \tilde{h}_i in a self-consistent manner. We present Eq. (47) again:

$$-\frac{d\phi_i}{d\tau} + \omega_i - \tilde{\Omega} = \sin \phi_i \tilde{h}_i^R - \cos \phi_i \tilde{h}_i^I. \quad (106)$$

On the other hand, local field h_i is given by

$$h_i e^{-i\beta_0} = \xi_i^1 m^1 + z_i^A + z_i^G + |\Gamma| \exp(i\psi) s_i, \quad (107)$$

$$\psi = \text{Arg}(\Gamma). \quad (108)$$

Substituting Eq. (107) into Eq. (39), we obtain

$$\begin{aligned} -\frac{d\phi_i}{d\tau} + \omega_i - \Omega &= \sin \phi_i (\text{Re}[e^{i\beta_0} (\xi_i^1 m^1 + z_i^A + z_i^G)] + |\Gamma| \cos(\phi_i + \psi + \beta_0)) \\ &\quad - \cos \phi_i (\text{Im}[e^{i\beta_0} (\xi_i^1 m^1 + z_i^A + z_i^G)] + |\Gamma| \sin(\phi_i + \psi + \beta_0)) \\ &= \sin \phi_i \text{Re}[e^{i\beta_0} (\xi_i^1 m^1 + z_i^A + z_i^G)] \\ &\quad - \cos \phi_i \text{Im}[e^{i\beta_0} (\xi_i^1 m^1 + z_i^A + z_i^G)] - |\Gamma| \sin(\psi + \beta_0). \end{aligned} \quad (109)$$

Comparing Eq. (106) with Eq. (109), we can determine effective local field \tilde{h}_i :

$$\tilde{h}_i e^{-i\beta_0} = \xi_i^1 m^1 + z_i^A + z_i^G, \quad (110)$$

and we can obtain $\tilde{\Omega}$, which is the renormalized version of Ω :

$$\tilde{\Omega} = \Omega - |\Gamma| \sin(\psi + \beta_0). \quad (111)$$

These final two results are consistent with the first assumption for a pure effective local field \tilde{h}_i in Eq. (46).

Finally, we combine the results obtained from SK theory and SCSNA. We can safely replace $X(h_i, \omega_i - \Omega, \tau)$ of order parameters m^1 and U with Eq. (81) based on \tilde{h}_i :

$$\begin{aligned} m^1 &= \frac{1}{N} \sum_i \bar{\xi}_i^1 X(h_i, \omega_i - \Omega, \tau) \\ &= \frac{1}{N} \sum_i \bar{\xi}_i^1 \left\langle s_i(\tilde{h}_i) \right\rangle_{\omega_i} \end{aligned} \quad (112)$$

$$\begin{aligned} U &= \frac{1}{N} \sum_i \frac{\partial X(h_i, \omega_i - \Omega, \tau)}{\partial h_i} \\ &= \frac{1}{N} \sum_i \frac{\partial \left\langle s_i(\tilde{h}_i) \right\rangle_{\omega_i}}{\partial \tilde{h}_i}, \end{aligned} \quad (113)$$

$$\tilde{h}_i e^{-i\beta_0} = \xi_i^1 m^1 + z_i^A + z_i^G, \quad (114)$$

because \tilde{h}_i is independent of any microscopic configuration of unit i . In conclusion, we can obtain the order parameter equations (54) and (55). In this way, our derivation process is complete in a self-consistent manner.

- [1] C. Meunier, *Biol. Cybern.* **67**, 155 (1992).
- [2] D. Hansel, G. Mato, and C. Meunier, *Europhysics Letters* **23**, 367 (1993).
- [3] G. B. Ermentrout, *Journal of Mathematical Biology* **6**, 327 (1981).
- [4] H. Sakaguchi and Y. Kuramoto, *Pro. of Theo. Phys.* **76**, 576 (1986).
- [5] M. Mezard, G. Parisi, and M. A. Virasoro, *Spin glass theory and beyond* (World Scientific, 1987).
- [6] M. Shiino and T. Fukai, *J. Phys. A* **23**, L1009 (1990).
- [7] C. J. Perez and F. Ritort, *J. Phys. A* **30**, 8095 (1997).
- [8] M. Shiino and T. Fukai, *J. Phys. A* **25**, L375 (1992).
- [9] T. Aonishi, K. Kurata, and M. Okada, *Phys. Rev. Let.* **82**, 2800 (1999).
- [10] M. Yoshioka and M. Shiino, *Phys. Rev. E* **61**, 4732 (2000).
- [11] H. Sompolinsky, *Heidelberg Colloquium on Glassy Dynamics* (Springer-Verlag, 1987), pp. 485–527.
- [12] T. Aoyagi and K. Kitano, *Phys. Rev. E* **55**, 7424 (1997).

- [13] M. Okada, T. Fukai, and M. Shiino, Phys. Rev. E **57**, 2095 (1998).
- [14] H. Daido, Phys. Rev. Let. **68**, 1073 (1992).
- [15] Y. Kuramoto, *Chemical oscillations, waves and turbulence* (Springer-Verlag, 1984).
- [16] A. Arenas and C. J. P. Vicente, Europhys. Lett. **26**, 79 (1994).
- [17] L. L. Bonilla, C. J. P. Vicente, F. Ritort, and J. Soler, Phys. Rev. Let. **81**, 3643 (1998).
- [18] F. C. Hoppensteadt and E. M. Izhikevich, Phys. Rev. Let. **82**, 2983 (1999).
- [19] J. Cook, J. Phys. A **22**, 2057 (1989).
- [20] H. Daido, Phys. Rev. Let. **77**, 1406 (1996).
- [21] D. Sherrington and S. Kirkpatrick, Phys. Rev. Let. **35**, 1792 (1975).
- [22] T. Aonishi, Phys. Rev. E **58**, 4865 (1998).
- [23] T. Aoyagi and K. Kitano, Neural Computation **10**, 1527 (1998).
- [24] N. D. Mackenzie and A. P. Young, Phys. Rev. Let. **49**, 301 (1982).
- [25] G. Parisi, J. Phys. A. **13**, L115 (1980).
- [26] M. Mezard and M. A. Virasoro, J. Physique **46**, 1293 (1985).
- [27] R. Eckhorn, R. Bauer, W. Jordan, M. Brosch, W. Kruse, M. Munk, and H. J. Reitboeck, Biol. Cybern. **60**, 121 (1988).
- [28] C. M. Gray, P. König, A. K. Engel, and W. Singer, Nature **338**, 334 (1989).
- [29] W. A. Phillips and W. Singer, Behavioral and Brain Science **20**, 657 (1997).
- [30] W. J. Freeman and C. A. Sharda, Brain Res. Rev. **10**, 147 (1985).